DAMAGE ACCUMULATION IN COMPOSITE STRUCTURES UNDER REPEATED LOADS

Peter Shyprykevich[1], H. Thomas Hahn[2], Milan Mitrovic[2]

[1] *FAA William J. Hughes Technical Center*
AAR-430, Atlantic City Int'l Airport, NJ 08405, USA
[2] *Mechanical and Aerospace Engineering Department*
University of California at Los Angeles
Engineering IV, Los Angeles, CA 90095-1597, USA

SUMMARY: Results of an extensive testing program, which addressed the damage accumulation in composite structures under repeated loads, are described. The test program consisted of constant amplitude fatigue with and without preload, low-high and high-low constant amplitude blocks, various stress ratios, and a transport wing spectrum with and without elimination of low loads. Test coupons included unnotched, with center holes, and those with impact damage. These were selected to simulate damage initiation sites commonly found in composite aircraft structure. Threshold strain levels for damage initiation were established by constant amplitude testing, in terms of maximum strain amplitude or strain range, for the three damage initiation sites. The threshold strain data generated by constant amplitude loading was a reliable guideline in predicting damage accumulation under spectrum loading.

KEYWORDS: damage accumulation, repeated loads, composite laminates, spectrum fatigue, open hole damage, impact damage, threshold strain levels

INTRODUCTION

From the time advanced composites were introduced, accumulation of damage under repeated loads has been studied to determine residual strength and life. Based on a thorough literature search reported in Refs.1 to 3, it was judged that sufficient data were lacking to establish, with confidence, test protocols in the aircraft structure certification process and to develop a damage accumulation analysis methodology.

The main goal of the present study was to delineate the effects of various parameters defining spectrum loading on damage growth as a function of strain level. It was also important to define threshold strain levels below which fatigue damage does not accumulate so that the low-strain cycles could be eliminated from the spectrum or, if none of the load excursions are damaging, the fatigue testing can be eliminated all together. As these low-strain cycles are most numerous, a great amount of testing time can be reduced. (The number of cycles that defined lifetime of usage was set at 1 million, which is reasonable for aircraft structures but may not be for rotating parts). Once these effects are identified, one can accelerate fatigue testing by deleting appropriate loading parameters. For structures that are a mixture of

composites and metals, care must be taken when eliminating cycles that do not contribute to composite structure damage such that the metal structure is not compromised.

The test program consisted of constant amplitude fatigue with and without preload, low-high and high-low constant amplitude blocks, various stress ratios, and a transport wing spectrum with and without elimination of low loads. The purpose of the constant amplitude testing was to isolate damage scenarios. The purpose of full spectrum testing was to determine if what was learned in constant amplitude testing was translatable to more realistic scenarios and to validate damage accumulation models. Test coupons included unnotched, with center holes, and those with impact damage. These were selected to simulate damage initiation sites commonly found in composite aircraft structure. Different damage metrics were used for different types of specimens.

TEST PROCEDURES

All testing was conducted on 24- and 32-ply quasi-isotropic laminates made from AS4/3501-6 carbon/epoxy tape prepreg. Each ply was 0.13 mm thick. The lay-up of the 24-ply laminate was $[0/45/-45/90]_{s3}$ while the 32-ply laminate had two additional sublaminates of $[0/45/-45/90]_s$ lay-up. The 24-ply panels were used in tension-tension (T-T) fatigue while the 32-ply panels were used in tension-compression (T-C) and compression-compression (C-C) fatigue to prevent specimen buckling. All panels were made using the manufacturer's recommended cure cycle and inspected using an ultrasonic C-scan system. The panels were then cut into test specimens of various dimensions depending on the test condition. Table 1 lists specimen dimensions where L is specimen length, W is specimen width, and GL is gage length. Tension Transport Wing Standard Test Spectrum (TWIST) is a tension dominated fatigue spectrum, and Compression TWIST is a compression dominated fatigue spectrum. Notched specimens were simulated using a centrally located hole of 6.4 mm in diameter. The initial impact damage was ~12.7 mm in diameter.

Table 1: Specimen dimensions

		Unnotched			Open-Hole			Impact Damage		
		L	GL	W	L	GL	W	L	GL	W
T-T	24 ply	203(8)	76(3)	25(1)	153(6)	76(3)	38(1.5)	153(6)	51(2)	38(1.5)
T-C	32 ply	171(6.75)	44(1.75)	25(1)	140(5.5)	38(1.5)	38(1.5)	140(5.5)	38(1.5)	38(1.5)
C-C	32 ply	171(6.75)	25(1)	25(1)	140(5.5)	38(1.5)	38(1.5)	140(5.5)	38(1.5)	38(1.5)
TensionTWIST	24 ply				153(6)	76(3)	38(1.5)			
Compression TWIST	32 ply				140(5.5)	38(1.5)	38(1.5)	140(5.5)	38(1.5)	38(1.5)
Static Tension	24 ply	203(8)	76(3)	25(1)	203(8)	76(3)	38(1.5)	153(6)	51(2)	38(1.5)
Static Compression	32 ply	57(2.25)	38(1.5)	38(1.5)	57(2.25)	38(1.5)	38(1.5)	57(2.25)	38(1.5)	38(1.5)

all dimensions in mm
(in)

All testing was conducted in two servo-hydraulic load frames at ambient laboratory conditions using ASTM recommended loading rates. For static compression, an end-loaded compression test fixture, similar to the NASA short block compression test fixture, was used. Except for the static compression test specimens, all other specimens were tabbed with an aluminum sheet 3.2 mm thick. Fatigue testing was conducted mostly at a frequency of 10 Hz using load control. Fatigue load amplitudes were based on a percentage of static strength for a given type of specimen (unnotched, open-holed, impacted) and the predominant load direction (tension or compression). The static failure strains were obtained prior to fatigue testing and are listed

in Table 2. For unnotched coupons, strains were measured directly using strain gages. For the open-hole and impacted specimens, the strains were inferred from the unnotched failure strains using the appropriate strength reductions for each load direction.

Table 2: Static properties

	Unnotched	Open-Hole	Impact Damage
Ultimate tensile strength	UTS = 747 MPa	NTS = 407 MPa	
Ultimate compressive strength	UCS = 621 MPa	NCS = 352 MPa	CSAI = 470 MPa
Ultimate tensile strain	1.41 %	0.77 %	
Ultimate compressive strain	1.59 %	0.88 %	1.15 %

Spectrum Characteristics

TWIST was selected as representative of a typical repeated load regime to be experienced by a composite aircraft component. TWIST[4 ,5] consists of ten basic flights that are repeated to make a single block of 4,000 flights. Each block consists of ten stress ratio levels with the number of cycles at each level given in Table 3. For comparison purposes, two columns of R-ratios are shown, one for negative mean strain and one for positive mean strain. Note that each block consists of 398,665 cycles and 10 levels; this approximates the 4,000,000 cycles that are considered a lifetime number of flights (40,000) or, if a one-hour average flight time is assumed, 40,000 flight hours.

The occurrence of each load cycle within one flight and the flights within one block of TWIST are distributed randomly. However, in the present study, load cycles within one block were executed from the highest to the lowest excursions in order to understand the effect on damage propagation of the different load cycles. Initially, damage was measured by X-ray radiography after every second load level as is illustrated in Fig. 1. Later, the measurements were taken only after the second and fifth cycle.

Table 3: TWIST characteristics

Load level #	Multiplier and addition of flight mean	**R** [stress ratio] **(- mean strain)**	**R** [stress ratio] **(+ mean strain)**	N** [# of cycles]
1	1.60	-4.33	-0.23	1
2	1.50	-5.00	-0.20	2
3	1.30	-7.67	-0.13	5
4	1.15	-14.3	-0.07	18
5	0.99	199	0.01	52
6	0.84	11.5	0.09	152
7	0.68	5.25	0.19	800
8	0.53	3.26	0.31	4170
9	0.37	2.17	0.46	34800
10	0.22	1.56	0.64	358665

**N in this table represents # of cycles in 1 block of TWIST (4,000 flight hours), and it should be multiplied by 10 for full spectrum test (40,000 flight hours)

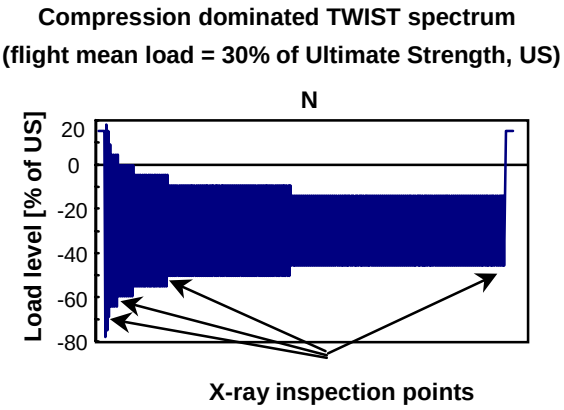

Fig 1: Graphical TWIST spectrum representation

Impact Damage

Impact damage was inflicted by a Dynatup 8200 drop weight impact testing machine with a 4.3-kg impactor having a 12.7-mm tup diameter. A modified SACMA SRM 2-88 [6] impact fixture was used to provide the necessary support for the specimens. Modifications were made to accommodate specimen dimensions used in this study such that a smaller 25.4- x 25.4-mm-square cutout was used instead of the recommended 76.2- x 127-mm cutout. In conjunction with the Dynatup machine, a model 730-I data acquisition and analysis system was used to provide complete records of impact energy and force as functions of time.

Initial impact tests were performed to determine the influence of impact test parameters on the damage development. Impact energy was adjusted to produce barely visible damage for subsequent fatigue loading. The overall impact damage area, in the form of a delamination, was determined using X-ray radiography and plotted versus the incident impact energy in Fig. 2. Caution should be taken when interpreting the maximum damage diameter of 25.4 mm, since it coincides with the 25.4- x 25.4-mm-square cutout of the clamping fixture. That is, the damage area might have been larger if a larger clamping fixture had been used.

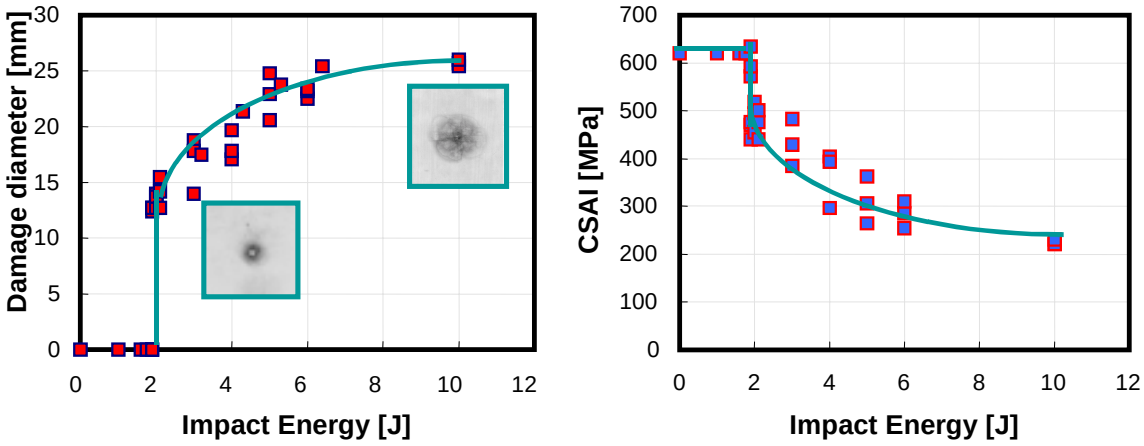

Fig.2: Damage diameter and compression strength after impact vs. incident impact energy

Compressive strengths and delamination sizes at different incident impact energy levels are shown in Fig. 2. Reduction in compressive strength closely follows the increase in delamination diameter. The average compression strength after impact (CSAI) of specimens without visible damage (600 MPa) is comparable to that of virgin specimens (621 MPa). Increasing impact energy slightly above the impact threshold level results in a CSAI of 470 MPa, which amounts to 25% reduction from the virgin strength. Since the objective of this research is to investigate the fatigue growth of barely visible impact damage (BVID), an incident impact energy of 2.1 J producing a repeatable delamination of ~12.7 mm in diameter was chosen for subsequent fatigue studies. The initial damage corresponded to a level consistent with the concept of BVID.

Damage Monitoring

Two methods were used to record the damage state: edge replication and X-ray radiography with zinc iodide (ZnI_2) penetrant. Edge replication was used to find ply cracks in all of the

unnotched T-T and T-C specimens and some of the open-hole specimens. At the end of each predetermined number of cycles, the specimen was loaded to approximately 0.3% strain and held there for a few minutes while the edge replicate was taken of the central 12.7-mm region of the specimen gage length. Ply cracking was measured by counting the crack imprints on the edge replicates. Only cracks extending through the entire ply thickness were counted and the data was then quantified in terms of crack density.

For impacted and open-hole specimens, and some unnotched specimens, ZnI_2-enhanced X-ray radiography was used to observe damage, particularly delaminations and splits. The X-ray radiography procedure is described in Ref. 2. The principal damage metric for coupons with a center holes was the length of a split that emanated from the hole edge. Damage progression in the specimens with impact damage was monitored in terms the maximum axial length of delamination area; although it was recognized that the extent of damage through the thickness of the laminate had a large influence on residual compressive strength.

TEST RESULTS

Unnotched Specimens

Test results for unnotched specimens are plotted in Fig. 3 in terms of crack density in 90° and -45° plies versus maximum strain level in T-T fatigue. The plotted values are average values of at least three coupons. During fatigue tests the load was kept constant; thus at a high number of cycles any decrease in stiffness and subsequent increase in strain was not reflected in these plots. This is a conservative assumption and is consistent with normal design practice where all calculations are based on initial stiffness values. The change in stiffness due to fatigue damage, as measured in these tests, varied from a few percent to a maximum of 10%, with the latter for cases where edge delaminations were severe.

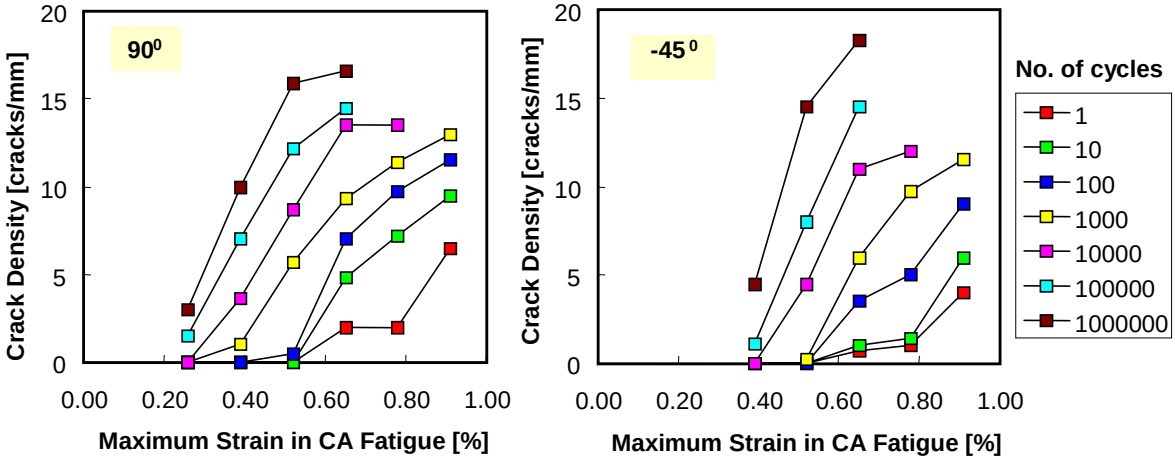

Fig. 3: Crack density in 90º and -45º plies for T-T fatigue

Figure 3 shows that the strain at which ply cracking initiated depends on the number of fatigue cycles. The greater the number of cycles the lower the strain level. The threshold strain for one cycle, essentially static load, is approximately 0.5% which correlates well with the failure strain levels obtained from transverse tension tests (90° plies). At one million cycles the strain levels below which there is no damage are about 0.2% for 90° plies and 0.3% for -45° plies. The static failure strain was measured as 1.41%. Thus the reduction from static strength to

fatigue runout is almost 85% for unnotched laminates. It should be noted that there is a saturation crack density of 17 cracks/mm after which the cracks tend to coalesce into delaminations at specimen edges. This type of damage mode is caused by the out-of-plane stresses due to the free edge and would only be representative of actual structure when such stresses exist.

Crack density data presented in Fig. 3 relates to T-T loading at R=0.1. At different stress ratios the general trend is the same as described before: the 90^o plies cracked first, followed by the -45^o plies. However, some differences were found in ply crack initiation and the final crack density. In T-T fatigue at R=0.1, ply crack initiation occurred earlier in both 90^o and -45^o plies than at other stress ratios (R=0.4, 0.6, and 0.8 with maximum strain of 0.78%) although the earlier crack initiation did not necessarily result in a higher crack density as fatigue cycles increased. That is, as fatigue continued, the stress ratio effect diminished, resulting in similar crack densities at 10^6 cycles for all stress ratios. These results suggest that in T-T fatigue the maximum tensile strain (ε_{max}) is more important than the strain range ($\Delta\varepsilon = \varepsilon_{max} - \varepsilon_{min}$) as far as the ply cracking is concerned. C-C fatigue regime did not cause any crack damage while the T-C fatigue regime resulted in accelerated edge delaminations that masked the increase in crack density.

Open-Hole Specimens

Constant Amplitude Fatigue

Damage growth in the form of splitting in open-holed specimens is plotted in Fig. 4. The strains in Fig. 4(a) are the average far-field maximum strains derived from load measurements. The type of damage observed and the measurement of split length are shown in the Fig. 4(a) inset. When replotted, in Fig. 4(b), using strain range, the same data (except at high-strain levels) collapses into one curve irrespective of whether the fatigue cycling was tension-tension, compression-compression, or tension-compression. That is, the initiation and growth of fiber splitting is a function of strain amplitude only. At higher fatigue strain levels in C-C fatigue (>0.52% strain), widthwise delamination extension and fiber failure in load bearing plies became dominant damage modes, retarding the split growth, and leading to laminate failure well before 10^6 cycles.

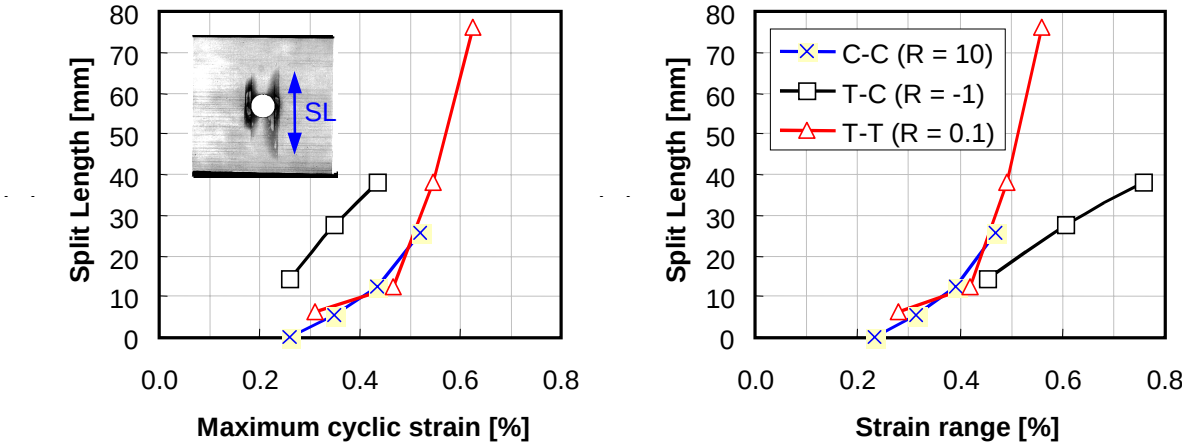

Fig. 4: Split damage at 10^6 cycles as a function of maximum fatigue strain (a) and strain range (b) in constant amplitude fatigue (T-Tension, C-Compression)

Spectrum Fatigue

Fatigue testing was done at three different flight mean loads in both tension and compression dominated TWIST spectrum. In Fig. 5(a), the split length after 10 blocks is plotted versus the strain range of the highest load excursion. Each point represents an average of six coupons: three specimens were tested under the full spectrum and the other three were tested in modified spectrum in which the two lowest load levels were omitted. It should be noted that the omission of low-load levels did not change average damage characteristics, suggesting that these two load levels (0.18%< strain range < 0.34%) can be omitted from the test sequence without significant influence on fatigue damage propagation. This conclusion is in line with the constant amplitude data which indicated that the threshold strain range was 0.2%.

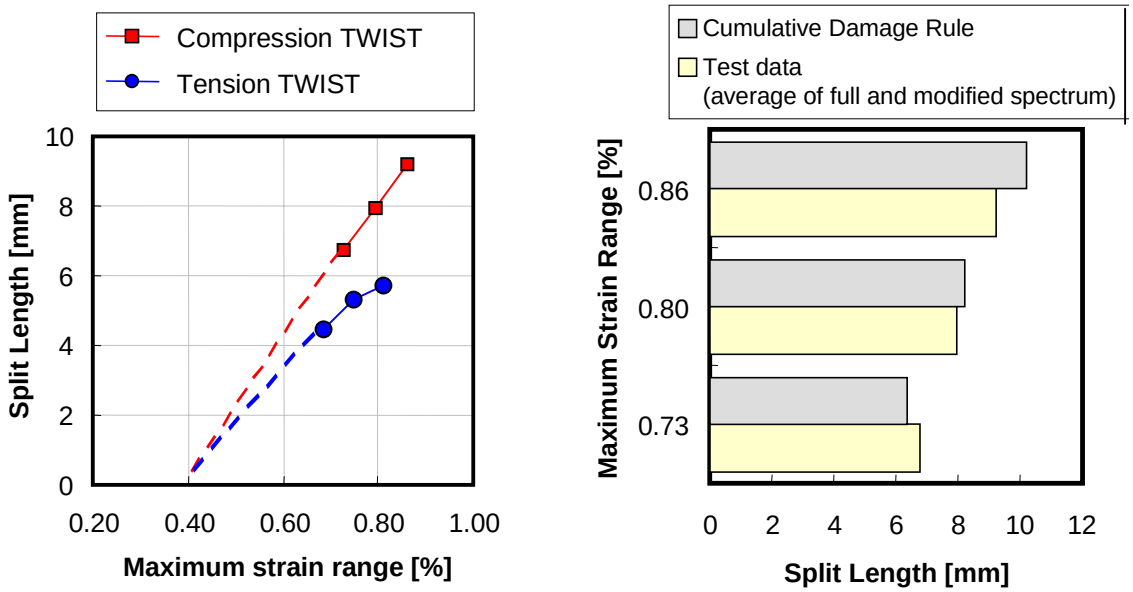

Fig. 5: Split damage after 10 blocks of TWIST as a function of maximum strain range: (a) comparison between tension and compression dominated spectrum, (b) cumulative damage model prediction for compression spectrum at three different load levels

Constant amplitude T-T fatigue at higher strains has resulted in larger split damage after 10^6 cycles than C-C loading (Fig. 4). On the other hand, in spectrum fatigue slightly smaller split damage was observed in tension dominated TWIST at higher strain levels as indicated in Fig. 5(a). However, the threshold strain range for both tension and compression spectrum is approximately the same, i.e., 0.4%. While this value is higher than the one observed in constant amplitude fatigue, it should be noted that within 10 blocks of TWIST the highest load level occurs only 10 times (see Table 3) while the other $4x10^6$ cycles have lower strain magnitude.

As stated earlier, the purpose of full spectrum testing was to determine if what was learned in constant amplitude fatigue was translatable to more realistic fatige regimes and to validate damage accumulation models. A comparison between observed split lengths and predictions from the linear history-independent cumulative damage model [7] is presented in Fig. 5(b). Split length data from the constant amplitude fatigue at different stress ratios were used to predict the damage growth during spectrum fatigue. For some lodings, the constant amplitude damage growth data were extrapolated for both strain range and maximum strain to better represent loading amplitudes and stress ratios present in the TWIST spectrum (Table 3).

Furthermore, the two lowest load levels were neglected in constructing this diagram. Therefore Fig. 5(b) applies to both full and modified spectrums. For lower strain levels reasonable agreement between test data and model prediction is obtained. It should be noted that in two-level block loading the low-high sequence resulted in longer splits than the high-low sequence, and the cumulative damage model was not able to predict this effect. However, in spectrum tests, sequence effect seems to diminish, leading to better correlation with model prediction. That is, although testing within one block was performed from highest to lowest load level (high-low load sequence indicated in Fig. 1), the same sequence was repeated 10 times such that the sequence effect should be pronounced only within the first block of loading.

Both constant amplitude and spectrum fatigue results indicate that a minimum threshold strain range can be established such that, if it is not exceeded in real usage, damage will not grow around open holes. The threshold strain range for damage initiation fatigue for the open-holed laminates tested is 0.2% for constant amplitude fatigue and 0.4% for spectrum fatigue. The static ultimate strain levels for the open-hole specimen were 0.77% for tension and 0.88% for compression. Thus the reduction for load cycling was much less for notched specimens than for unnotched laminates. It should be noted that the data was obtained for a quasi-isotropic laminate for which the stress concentration around the hole was ~3. For laminates that are more orthotropic, the threshold strain may be lower although prior work [8] has indicated that the stress concentration effects are much more pronounced for static strength than for high-cycle fatigue. This has also been shown by the work reported in this paper.

Impacted Specimens

Constant Amplitude Fatigue

A total of 64 impacted specimens were tested in constant amplitude T-T, T-C, and C-C fatigue. In T-T and T-C fatigue, impacted and unnotched specimens showed negligible difference in their *S-N* curves and damage growth modes as the predominant damage mode was tension dominated edge delamination not impact caused delamination. In C-C fatigue, the extent and mode of delamination growth varied significantly depending on the applied load level. In specimens cycled at 40% and 50% CSAI, the impact-induced damage did not grow up to 10^6 cycles (100% CSAI = 1.15% strain). At 60% CSAI, impact damage grew slightly in one specimen up to 10^6 cycles. At higher load levels, 70% and 80% CSAI, more severe damage growth was observed as shown on the right in Fig. 6. Thus, the threshold strain in constant amplitude C-C fatigue is 0.69% which represents only a 40% reduction from the static strength. However, overloads greater than 70% CSAI (0.8% strain) will trigger delamination growth due to local buckling even when the maximum compressive stress is reduced to 30% CSAI (i.e., high-low loading sequence). Delamination length as a function of maximum compressive stress for these cases is shown in Fig. 6. These results indicate the deleterious effect of high-load excursions on damage growth. That is, once delamination growth was initiated (separation of thin surface layer from the base laminate), forces required to extend the delamination further were substantially reduced from the forces required to initiate it. Therefore, fatigue design in the presence of BVID should focus on determination of high-load levels that initiate damage growth, because overloads can reduce the threshold strain for delamination growth to less than 0.3%. The observed delamination growth was only a few plies deep and did not have any effect on residual strength. However, in service the observed damge would trigger repair actions.

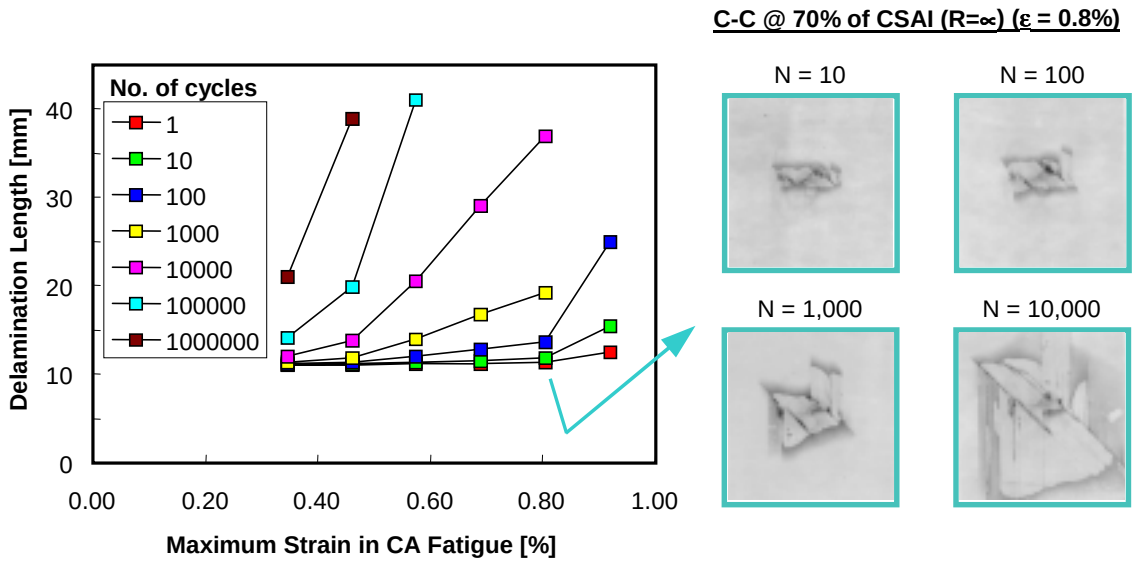

Fig.6: Axial delamination length in C-C loading (R=α) after a preload and and an example of damage growth in constant amplitude C-C loading at 70% CSAI

Spectrum Fatigue

A total of 18 specimens were tested under the TWIST spectrum, 9 specimens under the full spectrum loading and 9 specimens under the modified one with the two lowest load levels deleted. In both cases, the impact damage grew when the maximum compressive strains were at 0.83% and 0.9%. Specimens tested at the maximum strain of 0.75% did not exhibit any damage growth, and all survived 10 blocks of TWIST. These results are consistent with the aforementioned deleterious effects of high overloads on damage growth initiation. Damage patterns were similar in both full and modified spectrum fatigue. That is, delamination damage growth was only due to the high-load excursions and it was negligible at when the strain range was equal to or less than 0.23% and the maximum strain was below 0.3%.

CONCLUSIONS

1. Results from constant amplitude testing of coupons can be useful in determining whether full-scale fatigue testing is needed for certification, and if yes, they provide guidelines for the selection of economical and meaningful test spectrum loading content.

2. Damage progression in unnotched specimens begins with cracking of 90º plies and progresses with cracks in the ±45º plies. With no load reversal, crack density reaches a saturation point after which the damage switches to delamination if out-of-plane stresses exist. This was the case at the free edges of the specimens tested in tension. For positive R-ratios, crack accumulation was a function of the number and value of the maximum strain cycles. If the R-ratio was negative (i.e., load reversal), edge delaminations started much sooner and were the main damage characteristic. For matrix cracking, a threshold strain for no damage growth can be established as a function of maximum strain and number of cycles.

3. For laminates with a stress riser, in this case specimens with centrally located hole, damage progression consisted of longitudinal cracks emanating from the edge of the hole followed by delaminations. Damage characteristics around the hole were similar under tension

and compression loadings. Thus, a threshold strain level for no damage growth could be established as a function of strain range.

4. Damage progression of impacted specimens under compressive cyclic loads was characterized by delamination growth of the dominant delamination near the backface of the specimen. A threshold strain for the growth of this delamination can be established. However, once these loads are exceeded the damage can grow susequently even at strains lower than the threshold strain. However, as the delamination was near the surface the residual strength was not effected.

5. The threshold strain data generated during constant amplitude fatigue can serve as a guideline to determine the load levels that can be eliminated from spectrum loading. A comparison of damage growth in full and modified spectrums indicated that the two lowest load levels of TWIST spectrum (which represent 98.69% of testing time) could be deleted without any significant influence on damage propagation and fatigue life. For the quasi-isotropic specimens tested, the threshold load levels for no damage growth correspond to a strain range of 0.2% and a maximum fatigue strain of 0.3% for both open-holed and BVID impacted specimens.

6. The threshold strains for no damage growth obtained here should be used with caution as they may be dependent on the material and laminate stacking sequence, the latter particularly for delamination growth.

REFERENCES

1. Hahn, H.T., J. Timmer, J. Bartley-Cho, and S.G. Lim, *The Effect of Preloading on Fatigue Damage in Composite Structures: Part I*, DOT/FAA/AR-95/79, April 1996.

2. Hahn, H.T., J. Bartley-Cho, and S.G. Lim, *The Effect of Loading Parameters on Fatigue of Composite Laminates: Part II*, DOT/FAA/AR-96/76, July 1997.

3. Hahn, H.T., Mitrovic M., and Turkgenc, O., *The Effect of Loading Parameters on Fatigue of Composite Laminates: Part III*, DOT/FAA/AR-98/76, July 1999.

4. Phillips, E.P., "Effects of Truncation of a Predominantly Compression Load Spectrum on the Life of a Notched Graphite/Epoxy Laminate," *Fatigue of Fibrous Composite Materials, ASTM STP 723*, K.N. Lauraitis, ed., ASTM, (1981), pp. 197-212.

5. Schütz, D., "Variable Amplitude Fatigue Testing," *Agard Lecture Series, AGARD-LS-118* (1981), pp. 4/1-4/31.

6. SACMA Recommended Test Method for Compression After Impact Properties of Oriented Fiber-Resin Composites, SRM 2-88.

7. Hwang, W. and K.S. Han, "Cumulative Damage Models and Multi-Stress Fatigue Life Prediction," *Journal of Composite Materials*, **20**, (1986), pp. 125-153.

8. Schütz, D., Gerharz, J.J., and Alschweig, E., "The Fatigue Strength of Plain, Notched and Jointed Specimens of Carbon Fibre Composites," Royal Aircraft Establishment, Library Translation 2000, December 1978.